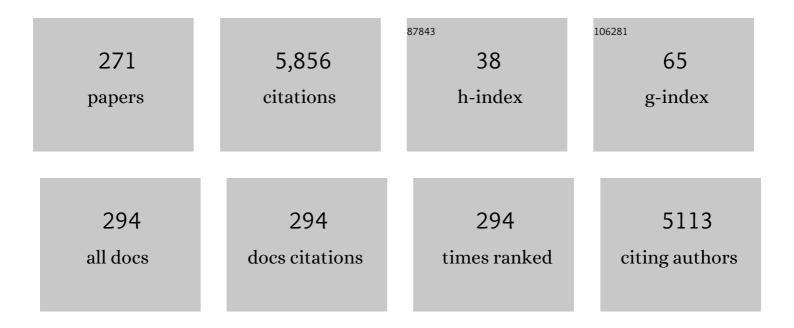
Guoyan Zheng

List of Publications by Year in descending order

Source: https://exaly.com/author-pdf/9179264/publications.pdf Version: 2024-02-01



#	Article	IF	CITATIONS
1	Spine-transformers: Vertebra labeling and segmentation in arbitrary field-of-view spine CTs via 3D transformers. Medical Image Analysis, 2022, 75, 102258.	7.0	27
2	MCG-Net: End-to-End Fine-Grained Delineation and Diagnostic Classification of Cardiac Events From Magnetocardiographs. IEEE Journal of Biomedical and Health Informatics, 2022, 26, 1057-1067.	3.9	2
3	Increased Combined Anteversion Is an Independent Predictor of Ischiofemoral Impingement in the Setting of Borderline Dysplasia With Coxa Profunda. Arthroscopy - Journal of Arthroscopic and Related Surgery, 2022, 38, 1519-1527.	1.3	4
4	CyCMIS: Cycle-consistent Cross-domain Medical Image Segmentation via diverse image augmentation. Medical Image Analysis, 2022, 76, 102328.	7.0	20
5	Entropy and distance maps-guided segmentation of articular cartilage: data from the Osteoarthritis Initiative. International Journal of Computer Assisted Radiology and Surgery, 2022, 17, 553-560.	1.7	4
6	Handling Imbalanced Data: Uncertainty-Guided Virtual Adversarial Training With Batch Nuclear-Norm Optimization for Semi-Supervised Medical Image Classification. IEEE Journal of Biomedical and Health Informatics, 2022, 26, 2983-2994.	3.9	5
7	Deep learning-based 2D/3D registration of an atlas to biplanar X-ray images. International Journal of Computer Assisted Radiology and Surgery, 2022, 17, 1333-1342.	1.7	9
8	What Factors Are Associated With Postoperative Ischiofemoral Impingement After Bernese Periacetabular Osteotomy in Developmental Dysplasia of the Hip?. Clinical Orthopaedics and Related Research, 2022, Publish Ahead of Print, .	0.7	4
9	Image-Less THA Cup Navigation in Clinical Routine Setup: Individual Adjustments, Accuracy, Precision, and Robustness. Medicina (Lithuania), 2022, 58, 832.	0.8	5
10	Nonlinear Regression via Deep Negative Correlation Learning. IEEE Transactions on Pattern Analysis and Machine Intelligence, 2021, 43, 982-998.	9.7	68
11	Frequency-Supervised MR-to-CT Image Synthesis. Lecture Notes in Computer Science, 2021, , 3-13.	1.0	6
12	MRI-based 3D models of the hip joint enables radiation-free computer-assisted planning of periacetabular osteotomy for treatment of hip dysplasia using deep learning for automatic segmentation. European Journal of Radiology Open, 2021, 8, 100303.	0.7	24
13	EquiSim: An Open-Source Articulatable Statistical Model of the Equine Distal Limb. Frontiers in Veterinary Science, 2021, 8, 623318.	0.9	2
14	A Projector-Based Augmented Reality Navigation System for Computer-Assisted Surgery. Sensors, 2021, 21, 2931.	2.1	10
15	DeepASDM: a Deep Learning Framework for Affine and Deformable Image Registration Incorporating a Statistical Deformation Model. , 2021, , .		1
16	2D/3D Registration with a Statistical Deformation Model Prior Using Deep Learning. , 2021, , .		3
17	Disentangled Representation Learning For Deep MR To CT Synthesis Using Unpaired Data. , 2021, , .		1
18	Guest Editorial Multi-Modal Computing for Biomedical Intelligence Systems. IEEE Journal of Biomedical and Health Informatics, 2021, 25, 3256-3257.	3.9	0

#	Article	IF	CITATIONS
19	Semantic Consistent Unsupervised Domain Adaptation for Cross-Modality Medical Image Segmentation. Lecture Notes in Computer Science, 2021, , 201-210.	1.0	14
20	Spine-Transformers: Vertebra Detection and Localization in Arbitrary Field-of-View Spine CT with Transformers. Lecture Notes in Computer Science, 2021, , 93-103.	1.0	8
21	Does the Rule of Thirds Adequately Detect Deficient and Excessive Acetabular Coverage?. Clinical Orthopaedics and Related Research, 2021, 479, 974-987.	0.7	10
22	Graphical User Interface for Joint Space Width Assessment by Optical Marker Tracking. , 2021, , .		0
23	Effect of pelvic tilt and rotation on cup orientation in standing anteroposterior radiographs. HIP International, 2020, 30, 48-55.	0.9	8
24	Editorial: Artificial Intelligence for Medical Image Analysis of Neuroimaging Data. Frontiers in Neuroscience, 2020, 14, 480.	1.4	7
25	Evaluation of an intensity-based algorithm for 2D/3D registration of natural knee videofluoroscopy data. Medical Engineering and Physics, 2020, 77, 107-113.	0.8	24
26	Evaluation of CTâ€MR image registration methodologies for 3D preoperative planning of forearm surgeries. Journal of Orthopaedic Research, 2020, 38, 1920-1930.	1.2	3
27	Entropy Guided Unsupervised Domain Adaptation for Cross-Center Hip Cartilage Segmentation from MRI. Lecture Notes in Computer Science, 2020, , 447-456.	1.0	8
28	Evaluation of algorithms for Multi-Modality Whole Heart Segmentation: An open-access grand challenge. Medical Image Analysis, 2019, 58, 101537.	7.0	180
29	Holistic decomposition convolution for effective semantic segmentation of medical volume images. Medical Image Analysis, 2019, 57, 149-164.	7.0	24
30	Novel adversarial semantic structure deep learning for MRI-guided attenuation correction in brain PET/MRI. European Journal of Nuclear Medicine and Molecular Imaging, 2019, 46, 2746-2759.	3.3	72
31	Patient-Specific 3-D Magnetic Resonance Imaging–Based Dynamic Simulation of Hip Impingement and Range of Motion Can Replace 3-D Computed Tomography–Based Simulation for Patients With Femoroacetabular Impingement: Implications for Planning Open Hip Preservation Surgery and Hip Arthroscopy, American Journal of Sports Medicine, 2019, 47, 2966-2977.	1.9	54
32	Femoroacetabular Impingement Patients With Decreased Femoral Version Have Different Impingement Locations and Intra- and Extraarticular Anterior Subspine FAI on 3D-CT–Based Impingement Simulation: Implications for Hip Arthroscopy. American Journal of Sports Medicine, 2019, 47, 3120-3132.	1.9	85
33	Fully Automatic Planning of Total Shoulder Arthroplasty Without Segmentation: A Deep Learning Based Approach. Lecture Notes in Computer Science, 2019, , 22-34.	1.0	3
34	Automated Recognition of Erector Spinae Muscles and Their Skeletal Attachment Region via Deep Learning in Torso CT Images. Lecture Notes in Computer Science, 2019, , 1-10.	1.0	7
35	Proof of concept: hip joint damage occurs at the zone of femoroacetabular impingement (FAI) in an experimental FAI sheep model. Osteoarthritis and Cartilage, 2019, 27, 1075-1083.	0.6	6
36	Standardized Assessment of Automatic Segmentation of White Matter Hyperintensities and Results of the WMH Segmentation Challenge. IEEE Transactions on Medical Imaging, 2019, 38, 2556-2568.	5.4	165

#	Article	IF	CITATIONS
37	Surgically Relevant Morphological Parameters of Proximal Human Femur: A Statistical Analysis Based on 3D Reconstruction of CT Data. Orthopaedic Surgery, 2019, 11, 135-142.	0.7	17
38	Benchmark on Automatic Six-Month-Old Infant Brain Segmentation Algorithms: The iSeg-2017 Challenge. IEEE Transactions on Medical Imaging, 2019, 38, 2219-2230.	5.4	136
39	Automatic MRI-based Three-dimensional Models of Hip Cartilage Provide Improved Morphologic and Biochemical Analysis. Clinical Orthopaedics and Related Research, 2019, 477, 1036-1052.	0.7	43
40	A Deep Learning Approach to Horse Bone Segmentation from Digitally Reconstructed Radiographs. , 2019, , .		4
41	Segmentation of the proximal femur in radial MR scans using a random forest classifier and deformable model registration. International Journal of Computer Assisted Radiology and Surgery, 2019, 14, 545-561.	1.7	26
42	Deep Volumetric Shape Learning for Semantic Segmentation of the Hip Joint from 3D MR Images. Lecture Notes in Computer Science, 2019, , 35-48.	1.0	1
43	3D Tiled Convolution for Effective Segmentation of Volumetric Medical Images. Lecture Notes in Computer Science, 2019, , 146-154.	1.0	8
44	Hybrid Generative Adversarial Networks for Deep MR to CT Synthesis Using Unpaired Data. Lecture Notes in Computer Science, 2019, , 759-767.	1.0	12
45	Automated Grading of Modic Changes Using CNNs – Improving the Performance with Mixup. Lecture Notes in Computer Science, 2019, , 41-52.	1.0	2
46	3D multi-scale FCN with random modality voxel dropout learning for Intervertebral Disc Localization and Segmentation from Multi-modality MR Images. Medical Image Analysis, 2018, 45, 41-54.	7.0	110
47	Augmented marker tracking for peri-acetabular osteotomy surgery. International Journal of Computer Assisted Radiology and Surgery, 2018, 13, 291-304.	1.7	20
48	Effect of Pelvic Tilt and Rotation on Cup Orientation in Both Supine and Standing Positions. Journal of Arthroplasty, 2018, 33, 1442-1448.	1.5	17
49	Crowd Counting with Deep Negative Correlation Learning. , 2018, , .		183
50	Novel deep learning-based CT synthesis algorithm for MRI-guided PET attenuation correction in brain PET/MR imaging. , 2018, , .		1
51	Why rankings of biomedical image analysis competitions should be interpreted with care. Nature Communications, 2018, 9, 5217.	5.8	198
52	Latent3DU-net: Multi-level Latent Shape Space Constrained 3D U-net for Automatic Segmentation of the Proximal Femur from Radial MRI of the Hip. Lecture Notes in Computer Science, 2018, , 188-196.	1.0	8
53	Bayesian VoxDRN: A Probabilistic Deep Voxelwise Dilated Residual Network for Whole Heart Segmentation from 3D MR Images. Lecture Notes in Computer Science, 2018, , 569-577.	1.0	26
54	Multi-object Model-Based Multi-atlas Segmentation Constrained Grid Cut for Automatic Segmentation of Lumbar Vertebrae from CT Images. Advances in Experimental Medicine and Biology, 2018, 1093, 65-71.	0.8	5

#	Article	IF	CITATIONS
55	Deep Learning-Based Automatic Segmentation of the Proximal Femur from MR Images. Advances in Experimental Medicine and Biology, 2018, 1093, 73-79.	0.8	12
56	3X-Knee: A Novel Technology for 3D Preoperative Planning and Postoperative Evaluation of TKA Based on 2D X-Rays. Advances in Experimental Medicine and Biology, 2018, 1093, 93-103.	0.8	2
57	Computer-Aided Orthopaedic Surgery: State-of-the-Art and Future Perspectives. Advances in Experimental Medicine and Biology, 2018, 1093, 1-20.	0.8	9
58	Computer-Assisted Planning, Simulation, and Navigation System for Periacetabular Osteotomy. Advances in Experimental Medicine and Biology, 2018, 1093, 143-155.	0.8	10
59	Biomechanical Optimization-Based Planning of Periacetabular Osteotomy. Advances in Experimental Medicine and Biology, 2018, 1093, 157-168.	0.8	4
60	Gravity-Assisted Navigation System for Total Hip Arthroplasty. Advances in Experimental Medicine and Biology, 2018, 1093, 181-191.	0.8	0
61	Atlas-Based 3D Intensity Volume Reconstruction from 2D Long Leg Standing X-Rays: Application to Hard and Soft Tissues in Lower Extremity. Advances in Experimental Medicine and Biology, 2018, 1093, 105-112.	0.8	2
62	How to Exploit Weaknesses in Biomedical Challenge Design and Organization. Lecture Notes in Computer Science, 2018, , 388-395.	1.0	10
63	Fully automatic segmentation of paraspinal muscles from 3D torso CT images via multi-scale iterative random forest classifications. International Journal of Computer Assisted Radiology and Surgery, 2018, 13, 1697-1706.	1.7	23
64	Statistical Shape Models and Atlases: Application to 2D-3D Reconstruction in THA. , 2018, , 183-190.		1
65	A novel technology for 3D knee prosthesis planning and treatment evaluation using 2D X-ray radiographs: a clinical evaluation. International Journal of Computer Assisted Radiology and Surgery, 2018, 13, 1151-1158.	1.7	13
66	Multi-scale Fully Convolutional DenseNets for Automated Skin Lesion Segmentation in Dermoscopy Images. Lecture Notes in Computer Science, 2018, , 513-521.	1.0	4
67	Fully automatic segmentation of lumbar vertebrae from CT images using cascaded 3D fully convolutional networks. , 2018, , .		62
68	Multi-stream 3D FCN with multi-scale deep supervision for multi-modality isointense infant brain MR image segmentation. , 2018, , .		26
69	DSMS-FCN: A Deeply Supervised Multi-scale Fully Convolutional Network for Automatic Segmentation of Intervertebral Disc in 3D MR Images. Lecture Notes in Computer Science, 2018, , 148-159.	1.0	5
70	Automatic Localization of the Lumbar Vertebral Landmarks in CT Images with Context Features. Lecture Notes in Computer Science, 2018, , 59-71.	1.0	2
71	Affinely Registered Multi-object Atlases as Shape Prior for Grid Cut Segmentation of Lumbar Vertebrae from CT Images. Lecture Notes in Computer Science, 2018, , 90-95.	1.0	0
72	In Vivo Quantification of the Deformations of the Femoropopliteal Segment. Journal of Endovascular Therapy, 2017, 24, 27-34.	0.8	26

#	Article	IF	CITATIONS
73	Optimising conservative management of chronic low back pain: study protocol for a randomised controlled trial. Trials, 2017, 18, 184.	0.7	18
74	Multi-atlas pancreas segmentation: Atlas selection based on vessel structure. Medical Image Analysis, 2017, 39, 18-28.	7.0	70
75	Effect of Stent Implantation on the Deformations of the Superficial Femoral Artery and Popliteal Artery: In Vivo Three-Dimensional Deformational Analysis from Two-Dimensional Radiographs. Journal of Vascular and Interventional Radiology, 2017, 28, 142-146.	0.2	9
76	3D U-net with Multi-level Deep Supervision: Fully Automatic Segmentation of Proximal Femur in 3D MR Images. Lecture Notes in Computer Science, 2017, , 274-282.	1.0	75
77	Augmented marker tracking for peri-acetabular osteotomy surgery. , 2017, 2017, 937-941.		4
78	A software program to measure the three-dimensional length of the spine from radiographic images: Validation and reliability assessment for adolescent idiopathic scoliosis. Computer Methods and Programs in Biomedicine, 2017, 138, 57-64.	2.6	4
79	Evaluation and comparison of 3D intervertebral disc localization and segmentation methods for 3D T2 MR data: A grand challenge. Medical Image Analysis, 2017, 35, 327-344.	7.0	59
80	Non-rigid free-form 2D–3D registration using a B-spline-based statistical deformation model. Pattern Recognition, 2017, 63, 689-699.	5.1	35
81	Statistical Shape and Deformation Models Based 2D–3D Reconstruction. , 2017, , 329-349.		8
82	Application of Image Processing Techniques in Molecular Imaging of Cancer. Contrast Media and Molecular Imaging, 2017, 2017, 1-2.	0.4	3
83	Atlas-Based 3D Intensity Volume Reconstruction of Musculoskeletal Structures in the Lower Extremity from 2D Calibrated X-Ray Images. Lecture Notes in Computer Science, 2017, , 35-43.	1.0	0
84	Fluoroscopy-based tracking of femoral kinematics with statistical shape models. International Journal of Computer Assisted Radiology and Surgery, 2016, 11, 757-765.	1.7	6
85	Fully automatic reconstruction of personalized 3D volumes of the proximal femur from 2D X-ray images. International Journal of Computer Assisted Radiology and Surgery, 2016, 11, 1673-1685.	1.7	23
86	Gaussian mixture models based 2D–3D registration of bone shapes for orthopedic surgery planning. Medical and Biological Engineering and Computing, 2016, 54, 1727-1740.	1.6	17
87	Computer Assisted Planning, Simulation and Navigation of Periacetabular Osteotomy. Lecture Notes in Computer Science, 2016, , 15-26.	1.0	1
88	Atlas-Based Reconstruction of 3D Volumes of a Lower Extremity from 2D Calibrated X-ray Images. Lecture Notes in Computer Science, 2016, , 366-374.	1.0	1
89	Patient-Specific 3D Reconstruction of a Complete Lower Extremity from 2D X-rays. Lecture Notes in Computer Science, 2016, , 404-414.	1.0	5
90	Statistical shape modeling of compound musculoskeletal structures around the thigh region. , 2016, ,		1

#	Article	IF	CITATIONS
91	A Cost-Effective Navigation System for Peri-acetabular Osteotomy Surgery. Lecture Notes in Computer Science, 2016, , 84-95.	1.0	2
92	Radiographic reconstruction of lower-extremity bone fragments: a first trial. International Journal of Computer Assisted Radiology and Surgery, 2016, 11, 2241-2251.	1.7	6
93	Constrained Statistical Modelling of Knee Flexion From Multi-Pose Magnetic Resonance Imaging. IEEE Transactions on Medical Imaging, 2016, 35, 1686-1695.	5.4	3
94	Independent Evaluation of a Mechanical Hip Socket Navigation System in Total Hip Arthroplasty. Journal of Arthroplasty, 2016, 31, 658-661.	1.5	2
95	Periacetabular osteotomy through the pararectus approach: technical feasibility and control of fragment mobility by a validated surgical navigation system in a cadaver experiment. International Orthopaedics, 2016, 40, 1389-1396.	0.9	16
96	Fully Automatic Segmentation of Hip CT Images. Lecture Notes in Computational Vision and Biomechanics, 2016, , 91-110.	0.5	2
97	A cost-effective surgical navigation solution for periacetabular osteotomy (PAO) surgery. International Journal of Computer Assisted Radiology and Surgery, 2016, 11, 271-280.	1.7	24
98	Automated 3D Lumbar Intervertebral Disc Segmentation from MRI Data Sets. Lecture Notes in Computational Vision and Biomechanics, 2016, , 25-40.	0.5	3
99	Fully Automatic Localization and Segmentation of Intervertebral Disc from 3D Multi-modality MR Images by Regression Forest and CNN. Lecture Notes in Computer Science, 2016, , 92-101.	1.0	4
100	Evaluation of Constant Thickness Cartilage Models vs. Patient Specific Cartilage Models for an Optimized Computer-Assisted Planning of Periacetabular Osteotomy. PLoS ONE, 2016, 11, e0146452.	1.1	23
101	Preoperative Planning of Periacetabular Osteotomy (PAO). Lecture Notes in Computational Vision and Biomechanics, 2016, , 151-171.	0.5	0
102	A Cost-Effective Surgical Navigation Solution for Periacetabular Osteotomy (PAO) Surgery. Lecture Notes in Computational Vision and Biomechanics, 2016, , 333-348.	0.5	1
103	Localization and Segmentation of 3D Intervertebral Discs from MR Images via a Learning Based Method: A Validation Framework. Lecture Notes in Computer Science, 2016, , 141-149.	1.0	0
104	Automated Intervertebral Disc Segmentation Using Deep Convolutional Neural Networks. Lecture Notes in Computer Science, 2016, , 38-48.	1.0	6
105	Fully Automatic Localization and Segmentation of 3D Vertebral Bodies from CT/MR Images via a Learning-Based Method. PLoS ONE, 2015, 10, e0143327.	1.1	86
106	Computer-Assisted Orthopedic Surgery: Current State and Future Perspective. Frontiers in Surgery, 2015, 2, 66.	0.6	92
107	Fully Automatic Segmentation of Hip CT Images via Random Forest Regression-Based Atlas Selection and Optimal Graph Search-Based Surface Detection. Lecture Notes in Computer Science, 2015, , 640-654.	1.0	0
108	Automated 3D Lumbar Intervertebral Disc Segmentation from MRI Data Sets. Lecture Notes in Computational Vision and Biomechanics, 2015, , 131-142.	0.5	1

#	Article	IF	CITATIONS
109	Personalized x-ray reconstruction of the proximal femur via a non-rigid 2D-3D registration. Proceedings of SPIE, 2015, , .	0.8	4
110	Cup Implant Planning Based on 2-D/3-D Radiographic Pelvis Reconstruction—First Clinical Results. IEEE Transactions on Biomedical Engineering, 2015, 62, 2665-2673.	2.5	10
111	Reconstruction of 3D Vertebral Models from a Single 2D Lateral Fluoroscopic Image. Lecture Notes in Computational Vision and Biomechanics, 2015, , 349-365.	0.5	2
112	Ruler Based Automatic C-Arm Image Stitching Without Overlapping Constraint. Journal of Digital Imaging, 2015, 28, 474-480.	1.6	12
113	What Are the Radiographic Reference Values for Acetabular Under- and Overcoverage?. Clinical Orthopaedics and Related Research, 2015, 473, 1234-1246.	0.7	250
114	Evaluation and Comparison of Anatomical Landmark Detection Methods for Cephalometric X-Ray Images: A Grand Challenge. IEEE Transactions on Medical Imaging, 2015, 34, 1890-1900.	5.4	135
115	FACTS: Fully Automatic CT Segmentation of a Hip Joint. Annals of Biomedical Engineering, 2015, 43, 1247-1259.	1.3	49
116	Which Radiographic Hip Parameters Do Not Have to Be Corrected for Pelvic Rotation and Tilt?. Clinical Orthopaedics and Related Research, 2015, 473, 1255-1266.	0.7	120
117	Localization and Segmentation of 3D Intervertebral Discs in MR Images by Data Driven Estimation. IEEE Transactions on Medical Imaging, 2015, 34, 1719-1729.	5.4	57
118	MASCG: Multi-Atlas Segmentation Constrained Graph method for accurate segmentation of hip CT images. Medical Image Analysis, 2015, 26, 173-184.	7.0	40
119	2D-3D regularized deformable b-spline registration: Application to the proximal femur. , 2015, , .		3
120	Medical image computing in diagnosis and intervention of spinal diseases. Computerized Medical Imaging and Graphics, 2015, 45, 99-101.	3.5	5
121	Biomechanical validation of computer assisted planning of periacetabular osteotomy: A preliminary study based on finite element analysis. Medical Engineering and Physics, 2015, 37, 1169-1173.	0.8	27
122	Patient-specific spinal stiffness in AIS: a preoperative and noninvasive method. European Spine Journal, 2015, 24, 249-255.	1.0	6
123	A complete-pelvis segmentation framework for image-free total hip arthroplasty (THA): methodology and clinical study. International Journal of Medical Robotics and Computer Assisted Surgery, 2015, 11, 166-180.	1.2	4
124	Non-rigid Free-Form 2D-3D Registration Using Statistical Deformation Model. Lecture Notes in Computer Science, 2015, , 102-109.	1.0	1
125	Comparison of 2.5D and 3D Quantification of Femoral Head Coverage in Normal Control Subjects and Patients with Hip Dysplasia. PLoS ONE, 2015, 10, e0143498.	1.1	17
126	Fully automatic segmentation of AP pelvis X-rays via random forest regression with efficient feature selection and hierarchical sparse shape composition. Computer Vision and Image Understanding, 2014, 126, 1-10.	3.0	6

#	Article	IF	CITATIONS
127	X-ray image calibration and its application to clinical orthopedics. Medical Engineering and Physics, 2014, 36, 968-974.	0.8	23
128	Statistical model-based segmentation of the proximal femur in digital antero-posterior (AP) pelvic radiographs. International Journal of Computer Assisted Radiology and Surgery, 2014, 9, 165-176.	1.7	14
129	Automatic X-ray landmark detection and shape segmentation via data-driven joint estimation of image displacements. Medical Image Analysis, 2014, 18, 487-499.	7.0	53
130	Is the acetabular cup orientation after total hip arthroplasty on a two dimension or three dimension model accurate?. International Orthopaedics, 2014, 38, 2009-2015.	0.9	34
131	Axial suspension test to assess pre-operative spinal flexibility in patients with adolescent idiopathic scoliosis. European Spine Journal, 2014, 23, 2619-2625.	1.0	12
132	Development of a balanced experimental–computational approach to understanding the mechanics of proximal femur fractures. Medical Engineering and Physics, 2014, 36, 793-799.	0.8	45
133	Articulated Statistical Shape Model-Based 2D-3D Reconstruction of a Hip Joint. Lecture Notes in Computer Science, 2014, , 128-137.	1.0	10
134	Computer Assisted Planning and Navigation of Periacetabular Osteotomy with Range of Motion Optimization. Lecture Notes in Computer Science, 2014, 17, 643-650.	1.0	25
135	3D Intervertebral Disc Localization and Segmentation from MR Images by Data-Driven Regression and Classification. Lecture Notes in Computer Science, 2014, , 50-58.	1.0	8
136	Image-Guided Orthopaedic Surgery. , 2014, , 647-659.		0
137	Fully Automatic CT Segmentation for Computer-Assisted Pre-operative Planning of Hip Arthroscopy. Lecture Notes in Computer Science, 2014, , 55-63.	1.0	0
138	Comparison of partial least squares regression and principal component regression for pelvic shape prediction. Journal of Biomechanics, 2013, 46, 197-199.	0.9	14
139	Pelvic Tilt Is Minimally Changed by Total Hip Arthroplasty. Clinical Orthopaedics and Related Research, 2013, 471, 417-421.	0.7	74
140	An Integrated System for 3D Hip Joint Reconstruction from 2D X-rays: A Preliminary Validation Study. Annals of Biomedical Engineering, 2013, 41, 2077-2087.	1.3	20
141	3D volumetric intensity reconsturction from 2D x-ray images using partial least squares regression. , 2013, , .		15
142	Fully Automatic Segmentation of AP Pelvis X-rays via Random Forest Regression and Hierarchical Sparse Shape Composition. Lecture Notes in Computer Science, 2013, , 335-343.	1.0	7
143	Expectation Conditional Maximization-Based Deformable Shape Registration. Lecture Notes in Computer Science, 2013, , 548-555.	1.0	5
144	Fully Automatic X-Ray Image Segmentation via Joint Estimation of Image Displacements. Lecture Notes in Computer Science, 2013, 16, 227-234.	1.0	1

#	Article	IF	CITATIONS
145	Robust Proximal Femur Segmentation in Conventional X-Ray Images via Random Forest Regression on Multi-resolution Gradient Features. Lecture Notes in Computer Science, 2013, , 442-450.	1.0	Ο
146	Evaluation of 3D correspondence methods for building point distribution models of the kidney. , 2012, , .		2
147	Calibration of C-arm for orthopedic interventions via statistical model-based distortion correction and robust phantom detection. , 2012, , .		10
148	Clinical experience with computer navigation in revision total hip arthroplasty. Proceedings of the Institution of Mechanical Engineers, Part H: Journal of Engineering in Medicine, 2012, 226, 919-926.	1.0	5
149	Determination of pelvic orientation from sparse ultrasound data for THA operated in the lateral position. International Journal of Medical Robotics and Computer Assisted Surgery, 2012, 8, 107-113.	1.2	5
150	Validation of a statistical shape model-based 2D/3D reconstruction method for determination of cup orientation after THA. International Journal of Computer Assisted Radiology and Surgery, 2012, 7, 225-231.	1.7	22
151	A multi-criteria decision support for optimal instrumentation in scoliosis spine surgery. Structural and Multidisciplinary Optimization, 2012, 45, 917-929.	1.7	5
152	Compensation of Sound Speed Deviations in 3-D B-Mode Ultrasound for Intraoperative Determination of the Anterior Pelvic Plane. IEEE Transactions on Information Technology in Biomedicine, 2012, 16, 88-97.	3.6	7
153	A Hierarchical Strategy for Reconstruction of 3D Acetabular Surface Models from 2D Calibrated X-Ray Images. Lecture Notes in Computer Science, 2012, , 74-83.	1.0	Ο
154	Scaled, patient-specific 3D vertebral model reconstruction based on 2D lateral fluoroscopy. International Journal of Computer Assisted Radiology and Surgery, 2011, 6, 351-366.	1.7	24
155	Kernel density correlation based non-rigid point set matching for statistical model-based 2D/3D reconstruction. , 2011, , .		Ο
156	Development of an auditory implant manipulator for minimally invasive surgical insertion of implantable hearing devices. Journal of Laryngology and Otology, 2011, 125, 262-270.	0.4	16
157	ECM versus ICP for point registration. , 2011, 2011, 2131-5.		1
158	Personalized X-Ray Reconstruction of the Proximal Femur via Intensity-Based Non-rigid 2D-3D Registration. Lecture Notes in Computer Science, 2011, 14, 598-606.	1.0	20
159	3D Model-based Reconstruction of the Proximal Femur from Low-dose Biplanar X-Ray Images. , 2011, , .		6
160	PS-GANS: A Patient-Specific, Gravity Assisted Navigation System for Acetabular Cup Placement. Lecture Notes in Computer Science, 2011, , 101-112.	1.0	1
161	Effective incorporating spatial information in a mutual information based 3D–2D registration of a CT volume to X-ray images. Computerized Medical Imaging and Graphics, 2010, 34, 553-562.	3.5	20
162	Assessing the Accuracy Factors in the Determination of Postoperative Acetabular Cup Orientation Using Hybrid 2D–3D Registration. Journal of Digital Imaging, 2010, 23, 769-779.	1.6	5

#	Article	IF	CITATIONS
163	Statistically Deformable 2D/3D Registration for Estimating Post-operative Cup Orientation from a Single Standard AP X-ray Radiograph. Annals of Biomedical Engineering, 2010, 38, 2910-2927.	1.3	20
164	An integrated approach for reconstructing a surface model of the proximal femur from sparse input data and a multi-resolution point distribution model: an in vitro study. International Journal of Computer Assisted Radiology and Surgery, 2010, 5, 99-107.	1.7	8
165	Computer assisted determination of acetabular cup orientation using 2D–3D image registration. International Journal of Computer Assisted Radiology and Surgery, 2010, 5, 437-447.	1.7	11
166	Validation of statistical shape model based reconstruction of the proximal femur—A morphology study. Medical Engineering and Physics, 2010, 32, 638-644.	0.8	33
167	Automated Intervertebral Disc Detection from Low Resolution, Sparse MRI Images for the Planning of Scan Geometries. Lecture Notes in Computer Science, 2010, , 10-17.	1.0	7
168	Statistical shape modeling of pathological scoliotic vertebrae: A comparative analysis. , 2010, 2010, 5939-42.		1
169	Statistical shape model-based reconstruction of a scaled, patient-specific surface model of the pelvis from a single standard AP x-ray radiograph. Medical Physics, 2010, 37, 1424-1439.	1.6	38
170	2D/3D reconstruction of a scaled lumbar vertebral model from a single fluoroscopic image. , 2010, 2010, 4395-8.		5
171	Automated detection of fiducial screws from CT/DVT volume data for image-guided ENT surgery. , 2010, 2010, 2325-8.		3
172	Determination of Pelvic Orientation from Ultrasound Images Using Patch-SSMs and a Hierarchical Speed of Sound Compensation Strategy. Lecture Notes in Computer Science, 2010, , 157-167.	1.0	7
173	Automated Vertebra Identification from X-Ray Images. Lecture Notes in Computer Science, 2010, , 1-9.	1.0	15
174	Development of a miniature robot for hearing aid implantation. , 2009, , .		3
175	MATCHING PARAMETERIZED SHAPES BY NONPARAMETRIC BELIEF PROPAGATION. International Journal of Pattern Recognition and Artificial Intelligence, 2009, 23, 209-246.	0.7	1
176	3D reconstruction of a patientâ€specific surface model of the proximal femur from calibrated xâ€ray	1.6	37
177	HipMatch: An object-oriented cross-platform program for accurate determination of cup orientation using 2D–3D registration of single standard X-ray radiograph and a CT volume. Computer Methods and Programs in Biomedicine, 2009, 95, 236-248.	2.6	22
178	Validation of a new method for determination of cup orientation in THA. Journal of Orthopaedic Research, 2009, 27, 1583-1588.	1.2	26
179	A novel parameter decomposition based optimization approach for automatic pose estimation of distal locking holes from single calibrated fluoroscopic image. Pattern Recognition Letters, 2009, 30, 838-847.	2.6	4
180	Robust automatic detection and removal of fiducial projections in fluoroscopy images: An integrated solution. Medical Engineering and Physics, 2009, 31, 571-580.	0.8	8

#	Article	IF	CITATIONS
181	Automatic extraction of proximal femur contours from calibrated X-ray images using 3D statistical models: an in vitro study. International Journal of Medical Robotics and Computer Assisted Surgery, 2009, 5, 213-222.	1.2	16
182	Landmarkâ€based augmented reality system for paranasal and transnasal endoscopic surgeries. International Journal of Medical Robotics and Computer Assisted Surgery, 2009, 5, 415-422.	1.2	20
183	A 2D/3D correspondence building method for reconstruction of a patient-specific 3D bone surface model using point distribution models and calibrated X-ray images. Medical Image Analysis, 2009, 13, 883-899.	7.0	132
184	Automatic extraction of proximal femur contours from calibrated X-ray images: a Bayesian inference approach. International Journal of Functional Informatics and Personalised Medicine, 2009, 2, 231.	0.4	0
185	Statistical Deformable Model-Based Reconstruction of a Patient-Specific Surface Model from Single Standard X-ray Radiograph. Lecture Notes in Computer Science, 2009, , 672-679.	1.0	4
186	Statistically Deformable 2D/3D Registration for Accurate Determination of Post-operative Cup Orientation from Single Standard X-ray Radiograph. Lecture Notes in Computer Science, 2009, 12, 820-827.	1.0	17
187	Calibration of a surgical microscope with automated zoom lenses using an active optical tracker. International Journal of Medical Robotics and Computer Assisted Surgery, 2008, 4, 87-93.	1.2	9
188	Radiographic analysis of femoroacetabular impingement with Hip ² norm—reliable and validated. Journal of Orthopaedic Research, 2008, 26, 1199-1205.	1.2	136
189	Comparison of Computer Assisted Surgery with Conventional Technique for Treatment of Abaxial Distal Phalanx Fractures in Horses: An In Vitro Study. Veterinary Surgery, 2008, 37, 32-42.	0.5	19
190	A Robust and Accurate Two-Stage Approach for Automatic Recovery of Distal Locking Holes in Computer-Assisted Intramedullary Nailing of Femoral Shaft Fractures. IEEE Transactions on Medical Imaging, 2008, 27, 171-187.	5.4	16
191	Automatic extraction of femur contours from calibrated x-ray images: A Bayesian inference approach. , 2008, , .		2
192	Calibration of X-ray radiographs and its feasible application for 2D/3D reconstruction of the proximal femur. , 2008, 2008, 470-3.		5
193	Robust automatic detection and removal of fiducial projections in fluoroscopy images: An integrated solution. , 2008, 2008, 78-81.		0
194	Landmark based augmented reality endoscope system for sinus and skull-base surgeries. , 2008, 2008, 74-7.		7
195	Robust intensity-based 3D-2D registration of ct and X-ray images for precise estimation of cup alignment after total hip arthroplasty. , 2008, , .		0
196	An Integrated Approach for Reconstructing a Surface Model of the Proximal Femur from Sparse Input Data and a Multi-Level Point Distribution Model. Lecture Notes in Computer Science, 2008, , 59-68.	1.0	0
197	Reality-augmented virtual fluoroscopy for computer-assisted diaphyseal long bone fracture osteosynthesis: A novel technique and feasibility study results. Proceedings of the Institution of Mechanical Engineers, Part H: Journal of Engineering in Medicine, 2008, 222, 101-115.	1.0	2
198	3-D reconstruction of a surface model of the proximal femur from digital biplanar radiographs. , 2008, 2008, 66-9.		9

#	Article	IF	CITATIONS
199	Automatic Extraction of Proximal Femur Contours from Calibrated X-Ray Images Using 3D Statistical Models. Lecture Notes in Computer Science, 2008, , 421-429.	1.0	4
200	Effective Incorporation of Spatial Information in a Mutual Information Based 3D-2D Registration of a CT Volume to X-Ray Images. Lecture Notes in Computer Science, 2008, 11, 922-929.	1.0	7
201	Automatic Mutual Nonrigid Registration of Dense Surfaces by Graphical Model Based Inference. Lecture Notes in Computer Science, 2008, , 694-704.	1.0	0
202	PRECISE POSE RECOVERY OF DISTAL LOCKING HOLES FROM SINGLE CALIBRATED FLUOROSCOPIC IMAGE VIA A NOVEL VARIABLE DECOMPOSITION APPROACH. , 2007, , .		0
203	Hardware accelerated ray cast of volume data and volume gradient for an optimized splines-based multi-resolution 2D-3D registration. , 2007, , .		0
204	A robust and accurate approach for reconstruction of patient-specific 3D bone models from sparse point sets. , 2007, , .		3
205	Automatic Extraction of Femur Contours from Calibrated Fluoroscopic Images. Proceedings IEEE Workshop on Applications of Computer Vision, 2007, , .	0.0	6
206	Hip2Norm: An object-oriented cross-platform program for 3D analysis of hip joint morphology using 2D pelvic radiographs. Computer Methods and Programs in Biomedicine, 2007, 87, 36-45.	2.6	72
207	Automated detection and segmentation of cylindrical fragments from calibrated C-arm images for long bone fracture reduction. Computer Methods and Programs in Biomedicine, 2007, 87, 1-11.	2.6	5
208	Accurate and Robust Reconstruction of a Surface Model of the Proximal Femur From Sparse-Point Data and a Dense-Point Distribution Model for Surgical Navigation. IEEE Transactions on Biomedical Engineering, 2007, 54, 2109-2122.	2.5	45
209	Integration of intraoperative imaging and surgical robotics to increase their acceptance. International Journal of Computer Assisted Radiology and Surgery, 2007, 1, 243-251.	1.7	2
210	OncoTREAT: a software assistant for cancer therapy monitoring. International Journal of Computer Assisted Radiology and Surgery, 2007, 1, 231-242.	1.7	35
211	(i) Registration techniques for computer navigation. Orthopaedics and Trauma, 2007, 21, 170-179.	0.3	43
212	Statistical deformable bone models for robust 3D surface extrapolation from sparse data. Medical Image Analysis, 2007, 11, 99-109.	7.0	102
213	Unsupervised Reconstruction of a Patient-Specific Surface Model of a Proximal Femur from Calibrated Fluoroscopic Images. , 2007, 10, 834-841.		13
214	Precise Estimation of Postoperative Cup Alignment from Single Standard X-Ray Radiograph with Gonadal Shielding. , 2007, 10, 951-959.		11
215	Automatic Extraction of Femur Contours from Calibrated X-Ray Images using Statistical Information. Journal of Multimedia, 2007, 2, .	0.3	9
216	New CAS Techniques in Trauma Surgery. , 2007, , 496-500.		0

#	Article	IF	CITATIONS
217	Advanced Technologies in Navigation. , 2007, , 582-585.		1
218	An Integrated Approach for Reconstructing Surface Models of the Proximal Femur from Sparse Input Data for Surgical Navigation. Lecture Notes in Computer Science, 2007, , 767-775.	1.0	0
219	Non-photorealistic rendering of virtual implant models for computer-assisted fluoroscopy-based surgical procedures. , 2007, , .		Ο
220	A CT-free, intra-operative planning and navigation system for minimally invasive anterior spinal surgery - an accuracy study. Computer Aided Surgery, 2007, 12, 233-241.	1.8	8
221	Incorporating Spatial Information into 3D-2D Image Registration. Lecture Notes in Computer Science, 2007, , 792-800.	1.0	0
222	Unifying Energy Minimization and Mutual Information Maximization for Robust 2D/3D Registration of X-Ray and CT Images. , 2007, , 547-557.		0
223	Accurate and reliable pose recovery of distal locking holes in computer-assisted intra-medullary nailing of femoral shaft fractures: A preliminary study. Computer Aided Surgery, 2007, 12, 138-151.	1.8	1
224	A Novel 3D/2D Correspondence Building Method for Anatomy-Based Registration. Lecture Notes in Computer Science, 2006, , 75-83.	1.0	10
225	Computerized fluoroscopy with zero-dose image updates for minimally invasive femoral diaphyseal fracture reduction. , 2006, , .		1
226	RANSAC-based EM algorithm for robust detection and segmentation of cylindrical fragments from calibrated C-arm images. , 2006, , .		0
227	An optimal three-stage method for anatomical shape reconstruction from sparse information using a dense surface point distribution model. , 2006, , .		Ο
228	Navigated open-wedge high tibial osteotomy: advantages and disadvantages compared to the conventional technique in a cadaver study. Knee Surgery, Sports Traumatology, Arthroscopy, 2006, 14, 917-921.	2.3	128
229	Computer Assisted Orthopaedic Surgery. International Journal of Computer Assisted Radiology and Surgery, 2006, 1, 229-250.	1.7	1
230	Minimal Invasive Spinal Surgery. International Journal of Computer Assisted Radiology and Surgery, 2006, 1, 189-200.	1.7	5
231	A Computational Framework for Automatic Determination of Morphological Parameters of Proximal Femur from Intraoperative Fluoroscopic Images. , 2006, , .		Ο
232	A Unifying MAP-MRF Framework for Deriving New Point Similarity Measures for Intensity-based 2D-3D Registration. , 2006, , .		5
233	An Optimized Spline-Based Registration of a 3D CT to a Set of C-Arm Images. International Journal of Biomedical Imaging, 2006, 2006, 1-12.	3.0	12
234	Assessment of splineâ€based 2D–3D registration for imageâ€guided spine surgery. Minimally Invasive Therapy and Allied Technologies, 2006, 15, 193-199.	0.6	15

#	Article	IF	CITATIONS
235	Reconstruction of Patient-Specific 3D Bone Surface from 2D Calibrated Fluoroscopic Images and Point Distribution Model. Lecture Notes in Computer Science, 2006, 9, 25-32.	1.0	43
236	Determining Geometrical Parameters by Particle Filter for Automatic Reconstruction of Surface Model of Proximal Femur from Biplanar Calibrated Fluoroscopic Images. , 2006, , .		0
237	Reconstruction of Patient-Specific 3D Bone Model from Biplanar X-Ray Images and Point Distribution Models. , 2006, , .		6
238	Use of a Dense Surface Point Distribution Model in a Three-Stage Anatomical Shape Reconstruction from Sparse Information for Computer Assisted Orthopaedic Surgery: A Preliminary Study. Lecture Notes in Computer Science, 2006, , 52-60.	1.0	15
239	Robust and Accurate Reconstruction of Patient-Specific 3D Surface Models from Sparse Point Sets: A Sequential Three-Stage Trimmed Optimization Approach. Lecture Notes in Computer Science, 2006, , 68-75.	1.0	7
240	Automatic Pose Recovery of the Distal Locking Holes from Single Calibrated Fluoroscopic Image for Computer-Assisted Intramedullary Nailing of Femoral Shaft Fractures. Lecture Notes in Computer Science, 2006, , 195-202.	1.0	1
241	Finding Deformable Shapes by Point Set Matching Through Nonparametric Belief Propagation. Lecture Notes in Computer Science, 2006, , 60-67.	1.0	Ο
242	Zero-dose fluoroscopy-based close reduction and osteosynthesis of diaphyseal fracture of femurs. Studies in Health Technology and Informatics, 2006, 119, 592-4.	0.2	1
243	Tilt and Rotation Correction of Acetabular Version on Pelvic Radiographs. Clinical Orthopaedics and Related Research, 2005, &NA, 182-190.	0.7	264
244	Navigated intraoperative analysis of lower limb alignment. Archives of Orthopaedic and Trauma Surgery, 2005, 125, 531-535.	1.3	57
245	A fluoroscopy-based surgical navigation system for high tibial osteotomy. Technology and Health Care, 2005, 13, 469-483.	0.5	17
246	Novel method for registering an endoscope in an operative setup. , 2005, 2005, 4349-52.		4
247	Kernel Regularized Bone Surface Reconstruction from Partial Data Using Statistical Shape Model. , 2005, 2005, 6579-82.		2
248	Automated Detection and Segmentation of Diaphyseal Bone Fragments From Registered C-Arm Images for Long Bone Fracture Reduction. , 2005, 2005, 4361-4.		2
249	Endoscope-based hybrid navigation system for minimally invasive ventral spine surgeries. Computer Aided Surgery, 2005, 10, 351-356.	1.8	13
250	Implementation, accuracy evaluation, and preliminary clinical trial of a CT-free navigation system for high tibial opening wedge osteotomy. Computer Aided Surgery, 2005, 10, 73-86.	1.8	38
251	Implementation, accuracy evaluation, and preliminary clinical trial of a CT-free navigation system for high tibial opening wedge osteotomy. Computer Aided Surgery, 2005, 10, 73-86.	1.8	7
252	Endoscope-based hybrid navigation system for minimally invasive ventral spine surgeries. Computer Aided Surgery, 2005, 10, 351-356.	1.8	5

#	Article	IF	CITATIONS
253	New orthopaedic implant management tool for computer-assisted planning, navigation, and simulation: From implant CAD files to a standardized XML-based implant database. Computer Aided Surgery, 2005, 10, 311-319.	1.8	3
254	Computer-assisted LISS plate osteosynthesis of proximal tibia fractures: Feasibility study and first clinical results. Computer Aided Surgery, 2005, 10, 141-149.	1.8	6
255	A fluoroscopy-based surgical navigation system for high tibial osteotomy. Technology and Health Care, 2005, 13, 469-83.	0.5	6
256	Computer aided high tibial open wedge osteotomy. Injury, 2004, 35, 68-78.	0.7	124
257	C-arm based navigation in total hip arthroplasty—background and clinical experience. Injury, 2004, 35, 90-95.	0.7	58
258	Computer aided reduction and imaging. Injury, 2004, 35, 96-104.	0.7	22
259	A CT-Free Intraoperative Planning and Navigation System for High Tibial Dome Osteotomy. Lecture Notes in Computer Science, 2004, , 610-620.	1.0	0
260	A Hybrid CT-Free Navigation System for Total Hip Arthroplasty. Computer Aided Surgery, 2002, 7, 129-145.	1.8	79
261	A hybrid CT-free navigation system for total hip arthroplasty. Computer Aided Surgery, 2002, 7, 129-145.	1.8	28
262	Frameless Optical Computer-Aided Tracking of a Microscope for Otorhinology and Skull Base Surgery. JAMA Otolaryngology, 2001, 127, 1233.	1.5	15
263	Multi-resolution elastic registration of CT and MR brain images. , 0, , .		0
264	Reconstruction of surfaces from contour data based on recursive medial axis of morphology-difference image and marching contour algorithm. , 0, , .		0
265	Surface Reconstruction of Bone from X-ray Images and Point Distribution Model Incorporating a Novel Method for 2D-3D Correspondence. , 0, , .		13
266	A Class of Novel Point Similarity Measures Based on MAP-MRF Framework for 2D-3D Registation of X-Ray Fluoroscopy to CT Images. , 0, , .		1
267	Augmented Marker Tracking for Peri-acetabular Osteotomy Surgery: A Cadaver Study. , 0, , .		1
268	Fully Automatic Segmentation and Landmarking of Hip CT Images. , 0, , .		0
269	3XPlan: A Novel Technology for 3D Prosthesis Planning Using 2D X-ray Radiographs. , 0, , .		0
270	Deep Learning based Segmentation of Lumbar Vertebrae from CT Images. , 0, , .		1

16

271 Projector-Based Augmented Reality System for Computer Assisted Orthonaedic Surgery 0	#	Article	IF	CITATIONS
	271	Projector-Based Augmented Reality System for Computer Assisted Orthopaedic Surgery. , 0, , .		1